Realization of the minimal extended seesaw mechanism and the TM_2 type neutrino mixing

R. Krishnan,[a] **Ananya Mukherjee**[b] **and Srubabati Goswami**[b]

[a]*Saha Institute of Nuclear Physics,*
 1/AF Bidhannagar, Kolkata 700064, India

[b]*Physical Research Laboratory,*
 Ahmedabad 380009, India

 E-mail: krishnan.rama@saha.ac.in, ananya@prl.res.in, sruba@prl.res.in

ABSTRACT: We construct a neutrino mass model based on the flavour symmetry group $A_4 \times C_4 \times C_6 \times C_2$ which accommodates a light sterile neutrino in the minimal extended seesaw (MES) scheme. Besides the flavour symmetry, we introduce a U(1) gauge symmetry in the sterile sector and also impose CP symmetry. The vacuum alignments of the scalar fields in the model spontaneously break these symmetries and lead to the construction of the fermion mass matrices. With the help of the MES formulas, we extract the light neutrino masses and the mixing observables. In the active neutrino sector, we obtain the TM$_2$ mixing pattern with non-zero reactor angle and broken μ-τ reflection symmetry. We express all the active and the sterile oscillation observables in terms of only four real model parameters. Using this highly constrained scenario we predict $\sin^2 \theta_{23} = 0.545^{+0.003}_{-0.004}$, $\sin \delta = -0.911^{+0.006}_{-0.005}$, $|U_{e4}|^2 = 0.029^{+0.009}_{-0.008}$, $|U_{\mu4}|^2 = 0.010^{+0.003}_{-0.003}$ and $|U_{\tau4}|^2 = 0.006^{+0.002}_{-0.002}$ which are consistent with the current data.

Contents

1 Introduction

Observations made in the neutrino oscillation experiments have confirmed that neutrinos have mass, albeit tiny. The Standard Model (SM) of particle physics can not accommodate the neutrino mass due to the absence of right-handed neutrinos, unlike the case for the charged leptons and the quarks. The inclusion of additional right-handed neutrino fields along with the seesaw mechanism [1–4] plays a vital role in modeling properties of massive neutrinos. The well known PMNS matrix encodes the mixing between the neutrino flavour eigenstates and their mass eigenstates. This matrix is parametrised in terms of three mixing angles and three CP phases (in a three flavoured paradigm),

$$
U_{\text{PMNS}} = \begin{pmatrix} c_{12}c_{13} & s_{12}c_{13} & s_{13}e^{-i\delta} \\ -s_{12}c_{23} - c_{12}s_{23}s_{13}e^{i\delta} & c_{12}c_{23} - s_{12}s_{23}s_{13}e^{i\delta} & s_{23}c_{13} \\ s_{12}s_{23} - c_{12}c_{23}s_{13}e^{i\delta} & -c_{12}s_{23} - s_{12}c_{23}s_{13}e^{i\delta} & c_{23}c_{13} \end{pmatrix} . U_{\text{Maj}}, \qquad (1.1)
$$

where $c_{ij} = \cos\theta_{ij}$, $s_{ij} = \sin\theta_{ij}$. The diagonal matrix, $U_{\text{Maj}} = \text{diag}(1, e^{i\alpha}, e^{i(\beta+\delta)})$, contains the Majorana CP phases α, β which become observable if the neutrinos behave as Majorana particles.

Although the last two decades of neutrino oscillation experiments made tremendous progress in determining the three flavour mixing angles, efforts are underway to measure these parameters more precisely. We do not yet know whether the atmospheric mixing is maximal or not. If it is not, the octant of the atmospheric mixing angle, θ_{23}, is to be determined. Measurement of the Dirac CP phase, δ, will confirm CP violation in the leptonic sector and may explain the observed baryon asymmetry via leptogenesis. The

nature of the neutrinos, i.e. whether they are Dirac or Majorana, is still an open question which can not be settled with the help of the oscillation experiments. On the other hand, the observation of neutrino-less double-beta decays ($0\nu\beta\beta$) will establish the Majorana nature. Such decays are yet to be observed. The oscillation experiments have determined the mass-squared differences (solar: Δm_{21}^2 and atmospheric: Δm_{31}^2), but they are not sensitive to the absolute neutrino mass scale. Data from the Planck satellite provides an upper bound on the sum of neutrino masses, $\sum_i m_i \leq 0.16\,\text{eV}$ [5]. Experimental searches are also being made to directly measure the electron neutrino mass using the kinematics of beta decays. Recently, the KATRIN collaboration has announced its first result on the effective electron antineutrino mass using the tritium beta decay, $^3\text{H} \to {}^3\text{He} + e^- + \bar{\nu}_e$, and reported the upper bound for the effective antineutrino mass [6], $m_{\bar{\nu}_e} < 1.1\,\text{eV}$ at the 90% confidence level (CL).

Although the three flavour paradigm of neutrino oscillation is well established, there are some experimental results that motivate us to go beyond this and postulate the existence of one or more sterile neutrinos. This possibility has gained considerable attention in recent years. In principle, the presence of a fourth neutrino can impressively explain several sets of experimental anomalies. The first indication came from the LSND experiment which showed evidence of oscillation with mass scale $\sim \text{eV}^2$ [7, 8] in $\bar{\nu}_\mu$-$\bar{\nu}_e$ channel. Later MiniBooNE experiment also confirmed it [9, 10]. The *Reactor Anomaly* involves a deficit of reactor antineutrinos detected in short-baseline (¡500 m) experiments with recalculated neutrino fluxes [11–13]. The short-baseline neutrino oscillations can also explain the so-called *Gallium Anomaly* observed during the calibrations runs of the radiochemical experiments, GALLEX and SAGE. The ratio of the experimental flux to the theoretical estimate was found to be 0.86 ± 0.05. The resolution of both the Reactor and the Gallium anomalies with the help of the active-sterile oscillations point towards a common region of the parameter space with the sterile neutrino having mass in the $\sim \text{eV}$ scale [14–17].

The proposed sterile neutrino is an SM singlet which does not participate in the weak interactions, but they can mix with the active neutrinos enabling them to be probed in the oscillation experiments. The addition of a single sterile neutrino field leads to an oscillation parameter space consisting of a 4×4 unitary mixing matrix along with three independent mass-squared-differences. Among them, the prefered scenario, often called the 3+1 scheme [18–21], has three active neutrinos and one sterile neutrino in the sub-eV and eV scale respectively. The 2+2 scheme, in which two pairs of neutrino mass states differ by $\mathcal{O}(\text{eV})$, is not consistent with the solar and the atmospheric data [22]. The 1+3 scheme in which the three active neutrinos are in eV scale and the sterile neutrino is lighter than the active neutrinos is disfavored by cosmology. Therefore, in this paper, we assume the 3+1 scenario. The recently proposed Minimal Extended Seesaw (MES) [23, 24] has many appealing features. The active-sterile mixing obtained in MES is suppressed by the ratio of masses of the active and sterile sectors. With the active neutrino mass of the order of $\sim 0.01\,\text{eV}$ and the sterile neutrino mass of the order of eV, this suppression is consistent with the active-sterile mixing as observed in LSND and MiniBooNe.[1]

---

[1]The data from solar and atmospheric neutrino oscillations as well as oscillations observed in accelerator experiments like T2K, MINOS, NOvA and reactor experiments KamLAND and Daya-Bay, RENO, Double-Chooz etc. can be explained in terms of the three neutrino framework. Because dominant oscillations to

A large number of neutrino mass models based on discrete flavour symmetry groups have been proposed [25–28] in the last decade. These models generate various mixing patterns such as the well known tribimaximal mixing (TBM) [29–35]. Since the non-zero value of the reactor mixing angle [36–38] has ruled out TBM, one of the popular ways to achieve realistic mixings is through either its modifications or extensions [39–45]. Unlike the active-only mixing scenarios, realising the minimal extended type-I seesaw with the help of discrete groups is somewhat recent and limited [46–49]. It is in this context that we propose a model to implement the MES and obtain oscillation observables consistent with the latest experiments. Our model produces an extension of the TBM called the TM$_2$ [50–58] in which the second column of the TBM is preserved. We use $A_4 \times C_4$ as the flavour group for our model. We propose several scalar fields, often called the flavons, which couple with the charged-lepton fields as well as the various neutrino fields. The inherent properties of A_4 and C_4 as well as the residual symmetries of the vacuum alignments of the flavons, determine the structure and the symmetries of the mass matrices.

The content of this paper is organised as follows. The features of the MES scheme are outlined in section 2. In section 3, we briefly explain the representation theory of the flavour group and move on to construct the Yukawa Lagrangian based on the proposed flavon content of the model. We also assign Vacuum Expectation Values (VEVs) for these flavons. We justify our assignments of VEVs with the help of symmetries in appendix A. In section 4, the mass matrices are constructed in terms of the VEVs. We provide the formulae for various experimental observables as functions of the model parameters. In section 5, we compare these formulae with the experimental results and make predictions. We provide a representative set of model parameters in appendix B and numerically extract the values of the observables so as to verify the validity of the various approximations used in the paper. Finally, we conclude in section 6.

2 Minimal extended seesaw

In the Standard Model, the left-handed charged-lepton fields, $l_L = (e_L, \mu_L, \tau_L)^T$, and the neutrino fields, $\nu_L = (\nu_e, \nu_\mu, \nu_\tau)^T$, transform as the SU(2) doublet, $L = (\nu_L, l_L)^T$. They couple with the right-handed charged-lepton fields, $l_R = (e_R, \mu_R, \tau_R)^T$, to form the charged-lepton mass term,

$$\bar{L} y_l l_R H, \tag{2.1}$$

where y_l are the Yukawa couplings. In general, y_l is a 3×3 complex matrix. The electroweak symmetry is spontaneously broken when the Higgs acquires the VEV,

$$\langle H \rangle = (0, v)^T. \tag{2.2}$$

---

sterile neutrinos is disfavored as a solution to solar and atmospheric neutrino anomalies, the 2+2 picture is disfavored. In the 3+1 picture, the oscillations to sterile neutrinos is a sub-leading effect to the dominant 3 flavour oscillations and the 3 generation global fit results are not altered. The short baseline eV^2 oscillations can be explained using the One-mass-scale-Dominance approximation governed by Δm_{41}^2. However, there is a tension between observance of non-oscillation in disappearance experiments and observation of oscillation in LSND and MiniBOONE which makes the goodness of fit in the 3+1 picture worse.

Subsequently, the mass term, eq. (2.1), becomes

$$\bar{l}_L M_l l_R, \tag{2.3}$$

where $M_l = v y_l$ is the charged-lepton mass matrix.

In the type-I seesaw framework, we add extra right-handed neutrino fields, ν_R, to the SM. We may assume that three families of such fields exist, i.e. $\nu_R = (\nu_{R1}, \nu_{R2}, \nu_{R3})^T$. They couple with the left-handed fields, L, forming the Dirac neutrino mass term,

$$\bar{L} y_\nu \nu_R \tilde{H}, \tag{2.4}$$

where $\tilde{H} = i\sigma_2 H^*$. As a result of the Spontaneous Symmetry Breaking (SSB), this term becomes

$$\bar{\nu}_L M_D \nu_R, \tag{2.5}$$

where $M_D = v y_\nu$ is the Dirac neutrino mass matrix. The right-handed neutrino fields can couple with themselves resulting in the Majorana mass term,

$$\frac{1}{2} \bar{\nu}_R^c M_R \nu_R, \tag{2.6}$$

where M_R is the 3×3 Majorana neutrino mass matrix which is assumed to be at a very high scale in order to cause the seesaw suppression of the light neutrino masses. The canonical type-I seesaw can be extended to accommodate an eV-scale sterile neutrino at the cost of no fine-tuning of the Yukawa coupling. To implement this MES scheme we need to include an SM gauge singlet field, ν_s, which couples with the heavy neutrino fields, ν_R, leading to

$$\bar{\nu}_s^c M_s \nu_R, \tag{2.7}$$

where M_s is a 1×3 mass matrix. We assume that the coupling of the sterile field (ν_s) with itself as well as with the left-handed fields (L) is forbidden.

Combining eqs. (2.5), (2.6), (2.7), we obtain the Lagrangian containing the neutrino mass matrices relevant to the MES:

$$\mathcal{L}_\nu = \bar{\nu}_L M_D \nu_R + \bar{\nu}_s^c M_s \nu_R + \frac{1}{2} \bar{\nu}_R^c M_R \nu_R + \text{h.c.} \tag{2.8}$$

The Lagrangian, eq. (2.8), leads to the following 7×7 neutrino mass matrix in the $(\nu_L, \nu_s^c, \nu_R^c)$ basis:

$$M_\nu^{7\times7} = \begin{pmatrix} 0 & 0 & M_D \\ 0 & 0 & M_s \\ M_D^T & M_s^T & M_R \end{pmatrix}. \tag{2.9}$$

Being analogous to the canonical type I seesaw, the MES scheme allows us to have the hierarchical mass spectrum assuming $M_R \gg M_s > M_D$. The right-handed neutrinos are much heavier compared to the electroweak scale enabling them to be decoupled at the low scale. As a result, eq. (2.9) can be block diagonalized to obtain the effective neutrino mass matrix in the (ν_L, ν_s^c) basis,

$$M_\nu^{4\times4} = -\begin{pmatrix} M_D M_R^{-1} M_D^T & M_D M_R^{-1} M_s^T \\ M_s (M_R^{-1})^T M_D^T & M_s M_R^{-1} M_s^T \end{pmatrix}. \tag{2.10}$$

This particular type of model is a minimal extension of the type I seesaw in the sense that only an extra sterile field is added whose mass is also suppressed along with that of the three active neutrinos. Since $M_\nu^{7\times7}$ has rank 6 and subsequently $M_\nu^{4\times4}$ has rank three, the lightest neutrino state becomes massless.[2]

Assuming $M_s > M_D$, we may apply a further seesaw approximation on eq. (2.10) to get the active neutrino mass matrix,

$$M_\nu^{3\times3} \simeq M_D M_R^{-1} M_s^T (M_s M_R^{-1} M_s^T)^{-1} M_s M_R^{-1} M_D^T - M_D M_R^{-1} M_D^T. \qquad (2.11)$$

It is worth mentioning that the r.h.s. of eq. (2.11) remains non-vanishing since M_s is a row vector 1×3 rather than a square matrix. Under the approximation $M_s > M_D$, we also obtain the mass of the 4th mass eigenstate,[3]

$$m_4 \simeq M_s M_R^{-1} M_s^T. \qquad (2.12)$$

The charged-lepton mass matrix, M_l, eq. (2.3), is a 3×3 complex matrix in general. Its diagonalisation leads to the charged-lepton masses,

$$U_L M_l U_R^\dagger = \text{diag}(m_e, m_\mu, m_\tau), \qquad (2.13)$$

where U_L and U_R are unitary matrices. The low energy effective 3×3 neutrino mass matrix, $M_\nu^{3\times3}$, eq. (2.11), is complex symmetric. Its diagonalisation is given by

$$U_\nu^\dagger M_\nu^{3\times3} U_\nu^* = \text{diag}(m_1, m_2, m_3), \qquad (2.14)$$

where U_ν is a unitary matrix and m_1, m_2 and m_3 are the light neutrino masses.[4] Using U_L and U_ν, we obtain the 4×4 light neutrino mixing matrix,

$$U \simeq \begin{pmatrix} U_L(1 - \frac{1}{2}RR^\dagger)U_\nu & U_L R \\ -R^\dagger U_\nu & 1 - \frac{1}{2}R^\dagger R \end{pmatrix}, \qquad (2.15)$$

where the three-component column vector R is given by

$$R = M_D M_R^{-1} M_s^T (M_s M_R^{-1} M_s^T)^{-1}. \qquad (2.16)$$

U, eq. (2.15), relates the neutrino mass eigenstates with the neutrino flavour eigenstates,

$$U(\nu_1, \nu_2, \nu_3, \nu_4)^T = (\nu_e, \nu_\mu, \nu_\tau, \nu_s)^T, \qquad (2.17)$$

in the basis where the charged-lepton mass matrix is diagonal. From eq. (2.15), it is evident that the strength of the active-sterile mixing is governed by

$$U_L R = (U_{e4}, U_{\mu4}, U_{\tau4})^T. \qquad (2.18)$$

---

[2]If we want to accommodate more than one sterile neutrino at the eV scale, we need to increase the number of heavy neutrinos as well. Otherwise, more than one active neutrino becomes massless which is ruled out experimentally.

[3]Since the active-sterile mixing is small, the 4th mass eigenstate (ν_4) more or less corresponds to the sterile state (ν_s).

[4]In the MES framework, we have $m_1 = 0$.

	(1)	(12)(34)	(123)	(132)
1	1	1	1	1
ω	1	1	ω	$\bar{\omega}$
ω̄	1	1	$\bar{\omega}$	ω
3	3	−1	0	0

Table 1. The character table of the A_4 group. A_4 denotes the even permutations of four objects. The conjugacy class (12)(34) represents two inversions carried out in two separate pairs of objects. (123) and (132) represent two inversions carried out in a set of three objects in the forward sense and the backward sense respectively. **1** is the trivial representation. **ω** and **ω̄** are singlets transforming as $\omega = e^{i\frac{2\pi}{3}}$ and $\bar{\omega} = e^{-i\frac{2\pi}{3}}$ under (123) and (132). **3** represents the three-dimensional rotational symmetries of a regular tetrahedron.

Note that R is suppressed by the ratio $\mathcal{O}(M_D/M_s)$. The 3×3 mixing matrix involving the three active neutrinos, $(\nu_e, \nu_\mu, \nu_\tau)$, and the three lightest mass eigenstates, (ν_1, ν_2, ν_3), is often called the PMNS mixing matrix, U_{PMNS}. In MES models with active-sterile mixing, U_{PMNS} will not be unitary. It is given by the upper-left block of eq. (2.15),

$$U_{\text{PMNS}} = U_L U_\nu - \frac{1}{2} U_L R R^\dagger U_\nu. \tag{2.19}$$

The deviation of U_{PMNS} from unitarity, i.e. $-\frac{1}{2} U_L R R^\dagger U_\nu$, is suppressed by $\mathcal{O}(M_D^2/M_s^2)$.

3 Flavour structure of the model

We construct the model in the framework of the discrete group $A_4 \times C_4$. A_4, which is the smallest group with a triplet irreducible representation, has been studied extensively in the literature [32, 59–65]. Here we briefly mention the essential features of this group in the context of model building. A_4 is the rotational symmetry group of the regular tetrahedron. It has the group presentation,

$$\langle S, T \mid S^2 = T^3 = (ST)^3 = I \rangle. \tag{3.1}$$

A_4 has 12 elements which fall under four conjugacy classes. Its conjugacy classes and irreducible representations are listed in table 1.

For the triplet representation, **3**, we choose the following basis,

$$S = \begin{pmatrix} 1 & 0 & 0 \\ 0 & -1 & 0 \\ 0 & 0 & -1 \end{pmatrix}, \quad T = \begin{pmatrix} 0 & 1 & 0 \\ 0 & 0 & 1 \\ 1 & 0 & 0 \end{pmatrix}. \tag{3.2}$$

The representations **ω** and **ω̄** transform as ω and $\bar{\omega}$ respectively under the generator T and trivially under the generator S. The tensor product of two triplets, (x_1, x_2, x_3) and (y_1, y_2, y_3), leads to

$$\mathbf{1} \equiv x_1 y_1 + x_2 y_2 + x_3 y_3 \,, \tag{3.3}$$

$$\boldsymbol{\omega} \equiv x_1 y_1 + \bar{\omega} x_2 y_2 + \omega x_3 y_3 \,, \tag{3.4}$$

$$\bar{\boldsymbol{\omega}} \equiv x_1 y_1 + \omega x_2 y_2 + \bar{\omega} x_3 y_3 \,, \tag{3.5}$$

$$\mathbf{3}_s \equiv (x_2 y_3 + x_3 y_2, x_3 y_1 + x_1 y_3, x_1 y_2 + x_2 y_1)^T \,, \tag{3.6}$$

$$\mathbf{3}_a \equiv (x_2 y_3 - x_3 y_2, x_3 y_1 - x_1 y_3, x_1 y_2 - x_2 y_1)^T \,. \tag{3.7}$$

	L	e_R	μ_R	τ_R	ν_R	ν_s	ϕ_l	η	ϕ	ϕ_s	η_ν	H	H_s
A_4	**3**	**1**	**1**	**1**	**3**	**1**	**3**	**1**	**3**	**3**	**1**	**1**	**1**
C_4	1	1	1	1	$-i$	i	1	i	i	1	-1	1	1
C_6	$-\omega$	$-\omega$	$\bar\omega$	1	$-\omega$	$-\omega$	$-\omega$	1	1	$\bar\omega$	ω	1	$\bar\omega$
$C_2 \times \mathrm{U}(1)_s$	1	1	1	1	1	$e^{iq\theta}$	1	1	1	-1	1	1	$-1 \times e^{-iq\theta}$

Table 2. The particle content and their charges under the flavour group of the model.

The triplets $\mathbf{3}_s$ and $\mathbf{3}_a$, both of which transforming as $\mathbf{3}$ under A_4, are constructed as the symmetric and the antisymmetric products respectively of x and y.

We extend the SM particle sector by the inclusion of three right-handed neutrinos, $\nu_R = (\nu_{R1}, \nu_{R2}, \nu_{R3})^T$, a sterile neutrino ($\nu_s$), several flavon multiplets, ϕ_l, η, ϕ, ϕ_s, η_ν and a sterile sector Higgs, H_s. Along with the A_4 group, the model includes several Abelian discrete groups (C_4, C_6 and C_2) acting variously on these fields. We also introduce a gauge group, $\mathrm{U}(1)_s$, in the sterile sector. The field content of the model, along with the irreducible representations they belong to, are given in table 2.

From these field assignments, we obtain the following Yukawa Lagrangian:

$$
\begin{aligned}
\mathcal{L}_Y = {}& Y_\tau \bar{L} \frac{\phi_l}{\Lambda} \tau_R H + Y_\mu \bar{L} \frac{\phi_l^*}{\Lambda} \mu_R H + \bar{L} \frac{Q}{\Lambda^2} e_R H \\
& + Y_\eta \bar{L} \nu_R \frac{\eta}{\Lambda} \tilde{H} + Y_{\phi s} \left(\bar{L} \nu_R \right)_{\mathbf{3}s}^T \frac{\phi}{\Lambda} \tilde{H} + Y_{\phi a} \left(\bar{L} \nu_R \right)_{\mathbf{3}a}^T \frac{\phi}{\Lambda} \tilde{H} \\
& + Y_s \frac{\phi_s^T}{\Lambda} \bar{\nu}_s^c \nu_R H_s + Y_\nu \eta_\nu \bar{\nu}_R^c \nu_R
\end{aligned}
\tag{3.8}
$$

where Y_τ, Y_μ, Y_η, $Y_{\phi s}$, $Y_{\phi a}$, Y_s, and Y_ν are the Yukawa-like dimensionless coupling constants, Λ is the cut-off scale of the theory. $()_{\mathbf{3}s}$ and $()_{\mathbf{3}a}$ represent the symmetric and the antisymmetric tensor products given in eq. (3.6) and eq. (3.7) respectively. Q represents all the quadratic flavon terms forming a triplet under A_4 and an invariant under the rest of the flavour group. It consists of $(\phi_l^* \phi_l)_{\mathbf{3}s}$, $(\phi_l^* \phi_l)_{\mathbf{3}a}$, $(\phi_s^* \phi_s)_{\mathbf{3}s}$, $(\phi_s^* \phi_s)_{\mathbf{3}a}$, $(\phi^* \phi)_{\mathbf{3}s}$, $(\phi^* \phi)_{\mathbf{3}a}$, $\eta^* \phi$, $\eta \phi^*$ along with the corresponding Yukawa-like coupling constants. Besides the flavour symmetries, we also impose the CP symmetry at high energy scales where the Higgses and the flavons have not acquired their VEVs, i.e. all the Yukawa-like couplings in the Lagrangian are real. We also assume that these couplings are of the order of one.

In the above Lagrangian, the first three terms are responsible for the charged-lepton mass generation. Since ϕ_l, ϕ_l^* and Q transform as $-\omega$, $-\bar\omega$ and 1 under C_6, they couple with $\bar{L} \tau_R$, $\bar{L} \mu_R$ and $\bar{L} e_R$ (which transform as $-\bar\omega$, $-\omega$ and 1) respectively. The rest of the terms involve the right-handed neutrino triplet ν_R and they contribute to the neutrino mass generation. The terms in the second line of eq. (3.8) contain $\bar{L} \nu_R$ which transforms as $-i$ under C_4 and remains invariant C_6. The flavons ϕ and η, which transform as i under C_4 and remain invariant C_6, couple with $\bar{L} \nu_R$. These terms result in the Dirac mass matrix for the neutrinos. Under $A_4 \times C_4 \times C_6 \times C_2 \times \mathrm{U}(1)_s$, the term $\bar{\nu}_s^c \nu_R$ transforms as $\mathbf{3} \times 1 \times \bar\omega \times 1 \times e^{iq\theta}$. This term couples with ϕ_s and H_s which transform as $\mathbf{3} \times 1 \times \bar\omega \times -1 \times 1$ and $\mathbf{1} \times 1 \times \bar\omega \times -1 \times e^{-iq\theta}$ respectively and forms the sterile mass term. Finally, we have the

Majorana mass term consisting of $\bar{\nu}_R^c \nu_R$ coupled with the flavon η_ν. We may also construct the neutrino mass terms $(\bar{L}\tilde{H})(\tilde{H}^T L^c)\frac{Q_1}{\Lambda^3}$, $\bar{L}\nu_s \frac{Q_2}{\Lambda^3}\tilde{H}H_s$ and $\bar{\nu}_s^c \nu_s \frac{Q_3}{\Lambda^3}H_s^2$ where Q_1, Q_2 and Q_3 represent the quadratic flavon terms transforming as $1 \times \bar{\omega} \times 1$, $-i \times \omega \times -1$ and $-1 \times 1 \times 1$ respectively under $C_4 \times C_6 \times C_2$. Since these mass terms are heavily suppressed, we have not included them in the Lagrangian. In fact, a part of the reason for assigning the various Abelian charges to the flavons, table 2, is to ensure that this suppression occurs so that our model leads to the standard MES framework where these terms are assumed to vanish (the block of zeros in eq. (2.9)).

Like the SM Higgs, the other scalar fields in the model also acquire VEVs through SSB. We assign them the following values:

$$\langle \phi_l \rangle = v_l(1, \bar{\omega}, \omega)^T, \tag{3.9}$$

$$\langle \eta \rangle = v_\eta, \tag{3.10}$$

$$\langle \phi \rangle = v_\phi(0, -i, 0)^T, \tag{3.11}$$

$$\langle \phi_s \rangle = v_s(1, 0, 1)^T, \tag{3.12}$$

$$\langle \eta_\nu \rangle = v_\nu, \tag{3.13}$$

$$\langle H_s \rangle = v'. \tag{3.14}$$

The VEVs of the various flavons in the model break the discrete flavour group, $A_4 \times C_4 \times C_6 \times C_2$ in specific ways. In appendix A, we study the residual symmetries of these VEVs and describe how their alignments can be uniquely defined.

The VEV of the sterile Higgs (H_s) breaks the $U(1)_s$ gauge group and leads to a massive gauge boson. This particle can mediate the so-called secret interactions of the sterile neutrinos proposed in the cosmological context [66–68]. The VEV of the sterile Higgs is assumed to be an order of magnitude higher than the VEV of the SM Higgs, i.e. $v = 176\,\text{GeV}$, $v' \approx 2000\,\text{GeV}$. We also assume that the flavon VEVs are at a very high energy scale $v_x \approx 10^{10}\,\text{GeV}$ where v_x denotes v_l, v_η, v_ϕ, v_s and v_ν and that the cut-off scale $\Lambda \approx 10^{13}\,\text{GeV}$. Under these assumptions, we may calculate the scales of our mass terms (after SSB); $\bar{l}_L \tau_R$, $\bar{l}_L \mu_R$: $v\frac{v_l}{\Lambda} \approx 10^{-1}$, $\bar{l}_L e$: $v\frac{\mathcal{O}(v_x^2)}{\Lambda^2} \approx 10^{-4}$, $\bar{\nu}_L \nu_R$: $v\frac{\mathcal{O}(v_x)}{\Lambda} \approx 10^{-1}$, $\bar{\nu}_s^c \nu_R$: $v'\frac{v_s}{\Lambda} \approx 1$, $\bar{\nu}_R^c \nu_R$: $v_\nu \approx 10^{10}$, $\bar{\nu}_L \nu_L^c$: $v^2\frac{\mathcal{O}(v_x^2)}{\Lambda^3} \approx 10^{-15}$, $\bar{\nu}_L \nu_s$: $vv'\frac{\mathcal{O}(v_x^2)}{\Lambda^3} \approx 10^{-14}$ and $\bar{\nu}_s^c \nu_s$: $v'^2\frac{\mathcal{O}(v_x^2)}{\Lambda^3} \approx 10^{-13}$ where all the units are in GeV.

4 Mass matrices and observables

Substituting the Higgs VEV and the flavon VEVs in the Lagrangian for the charged-lepton sector (first line of eq. (3.8)), we obtain the charged-lepton mass matrix, eq. (2.3),

$$M_l = v\frac{\mathcal{O}(v_x^2)}{\Lambda^2}\begin{pmatrix} \mathcal{O}(1) & 0 & 0 \\ \mathcal{O}(1) & 0 & 0 \\ \mathcal{O}(1) & 0 & 0 \end{pmatrix} + v\frac{v_l}{\Lambda}\begin{pmatrix} 0 & Y_\mu & Y_\tau \\ 0 & \omega Y_\mu & \bar{\omega} Y_\tau \\ 0 & \bar{\omega} Y_\mu & \omega Y_\tau \end{pmatrix}. \tag{4.1}$$

This mass matrix is diagonalised using the transformation,

$$U_L M_l U_R^\dagger = \text{diag}(m_e, m_\mu, m_\tau), \tag{4.2}$$

where

$$U_L \simeq \frac{1}{\sqrt{3}} \begin{pmatrix} 1 & 1 & 1 \\ 1 & \bar{\omega} & \omega \\ 1 & \omega & \bar{\omega} \end{pmatrix}, \tag{4.3}$$

U_R is an unobservable unitary matrix and

$$m_e = v\frac{\mathcal{O}(v_x^2)}{\Lambda^2}, \quad m_\mu \simeq \sqrt{3}Y_\mu v\frac{v_l}{\Lambda}, \quad m_\tau \simeq \sqrt{3}Y_\tau v\frac{v_l}{\Lambda} \tag{4.4}$$

are the masses of the charged leptons. Here, the electron mass is suppressed by a factor of $\frac{v_x}{\Lambda} \approx 10^{-3}$ compared to the muon and the tau masses. This is similar to the Froggatt-Nielsen mechanism which was proposed to explain the hierarchy of the fermion masses. It can be shown that the error in the expression of U_L given in eq. (4.3) is of the order of $\frac{v_x^2}{\Lambda^2}$. The relative errors in the expressions of m_μ and m_τ given in eqs. (4.4) are also of the same order. These errors are very small and hence can safely be ignored. For a numerical verification, please refer to appendix B.

The terms in the second line of the Lagrangian, eq. (3.8), generate the Dirac mass matrix for the neutrinos. Substituting Higgs VEV and the VEVs of the flavons η and ϕ, eqs. (3.10), (3.11), in these terms, we obtain the Dirac neutrino mass matrix, eq. (2.5),

$$M_D = v\frac{1}{\Lambda} \begin{pmatrix} v_\eta Y_\eta & 0 & -iv_\phi(Y_{\phi s} - Y_{\phi a}) \\ 0 & v_\eta Y_\eta & 0 \\ -iv_\phi(Y_{\phi s} + Y_{\phi a}) & 0 & v_\eta Y_\eta \end{pmatrix}. \tag{4.5}$$

Substituting the VEV of ϕ_s, eq. (3.12), in the mass term for the sterile neutrino, $Y_s \bar{\nu}_R^c \nu_s \frac{\phi_s}{\Lambda} H_s$, we obtain the mass matrix representing the couplings between ν_s and ν_R, eq. (2.7),

$$M_s = v'\frac{v_s}{\Lambda}Y_s(1, 0, 1). \tag{4.6}$$

Finally, from the term $Y_\nu \eta_\nu \bar{\nu}_R^c \nu_R$, we obtain the mass matrix for the heavy right-handed neutrinos, eq. (2.6),

$$M_R = Y_\nu v_\nu I, \tag{4.7}$$

where I is the 3×3 identity matrix.

We implement the MES scheme, eq. (2.10), using the neutrino mass matrices, M_D, M_s, M_R, eqs. (4.5), (4.6), (4.7), and obtain the following effective neutrino mass matrix:

$$M_\nu^{4\times4} = \begin{pmatrix} m\begin{pmatrix} 1-(\kappa_s-\kappa_a)^2 & 0 & -2i\kappa_s \\ 0 & 1 & 0 \\ -2i\kappa_s & 0 & 1-(\kappa_s+\kappa_a)^2 \end{pmatrix} & \frac{\sqrt{mm_s}}{\sqrt{2}}\begin{pmatrix} 1-i(\kappa_s-\kappa_a) \\ 0 \\ 1-i(\kappa_s+\kappa_a) \end{pmatrix} \\ \frac{\sqrt{mm_s}}{\sqrt{2}}\begin{pmatrix} 1-i(\kappa_s-\kappa_a) & 0 & 1-i(\kappa_s+\kappa_a) \end{pmatrix} & m_s \end{pmatrix}, \tag{4.8}$$

where

$$m = \frac{v^2 v_\eta^2 Y_\eta^2}{Y_\nu v_\nu \Lambda^2}, \quad m_s = \frac{2v'^2 v_s^2 Y_s^2}{Y_\nu v_\nu \Lambda^2}, \quad \kappa_s = \frac{v_\phi Y_{\phi s}}{v_\eta Y_\eta}, \quad \kappa_a = \frac{v_\phi Y_{\phi a}}{v_\eta Y_\eta}. \tag{4.9}$$

Here, the mass m is suppressed by the very high value of v_ν ($\approx 10^{10}$ GeV) and also by the ratio $\frac{\Lambda^2}{v_\eta^2}$ ($\approx 10^6$). Hence, we obtain m at around 0.01 eV. The ratio $\frac{m}{m_s}$ relates the scale of the active sector of the neutrinos to that of the sterile sector and it is given by $\frac{m}{m_s} = \frac{v^2 v_\eta^2 Y_\eta^2}{2v'^2 v_s^2 Y_s^2}$. Since v' is assumed to be an order of magnitude higher than v, the ratio $\frac{m}{m_s}$ becomes small (≈ 0.01). As a result, we can use eq. 2.11 to obtain the effective 3×3 neutrino mass matrix,

$$M_\nu^{3\times3} = \frac{m}{2} \begin{pmatrix} (\kappa_s - \kappa_a - i)^2 & 0 & \kappa_a^2 - (\kappa_s - i)^2 \\ 0 & -2 & 0 \\ \kappa_a^2 - (\kappa_s - i)^2 & 0 & (\kappa_s + \kappa_a - i)^2 \end{pmatrix}. \tag{4.10}$$

Using the unitary matrix,

$$U_\nu = \frac{1}{\sqrt{2}\kappa} \begin{pmatrix} i + \kappa_s + \kappa_a & 0 & -i + \kappa_s - \kappa_a \\ 0 & i\sqrt{2}\kappa & 0 \\ i + \kappa_s - \kappa_a & 0 & i - \kappa_s - \kappa_a \end{pmatrix} \quad \text{with} \quad \kappa = \sqrt{(1 + \kappa_s^2 + \kappa_a^2)}, \tag{4.11}$$

we diagonalise $M_\nu^{3\times3}$, eq. (4.10),

$$U_\nu^\dagger M_\nu^{3\times3} U_\nu^* = m \, \text{diag}\left(0, 1, 1 + \kappa_s^2 + \kappa_a^2\right), \tag{4.12}$$

to obtain the light neutrino masses,

$$m_1 = 0, \quad m_2 = m, \quad m_3 = m(1 + \kappa_s^2 + \kappa_a^2). \tag{4.13}$$

Using the expressions of U_L and U_ν, eqs. (4.3), (4.11), we obtain the PMNS mixing matrix ($U_{\text{PMNS}} \simeq U_L U_\nu$,[5] eq. (2.19)) in terms of the parameters κ_s and κ_a,

$$U_{\text{PMNS}} \simeq \frac{1}{\sqrt{6}\kappa} \begin{pmatrix} 2(i + \kappa_s) & i\sqrt{2}\kappa & -2\kappa_a \\ (i + \kappa_s)(1 + \omega) + \kappa_a(1 - \omega) & i\sqrt{2}\kappa\bar{\omega} & (-i + \kappa_s)(1 - \omega) - \kappa_a(1 + \omega) \\ (i + \kappa_s)(1 + \bar{\omega}) + \kappa_a(1 - \bar{\omega}) & i\sqrt{2}\kappa\omega & (-i + \kappa_s)(1 - \bar{\omega}) - \kappa_a(1 + \bar{\omega}) \end{pmatrix}. \tag{4.14}$$

The absolute values of the elements of the middle column of this mixing matrix are equal to $\frac{1}{\sqrt{3}}$, i.e. the mixing has the TM$_2$ form. Note that the eigenvalue m should correspond to the second neutrino eigenstate because this eigenstate should remain unmixed with the others in order to obtain the TM$_2$ mixing, eq. (4.14). Therefore, the mass ordering should be either $(0, m, m(1 + \kappa_s^2 + \kappa_a^2))$ or $(m(1 + \kappa_s^2 + \kappa_a^2), m, 0)$. The second case is inconsistent with the experimental observation of $m_1 < m_2$ given that κ_s and κ_a are real parameters. Hence, the model predicts the normal ordering (the first case) of the light neutrino masses.

---

[5]U_{PMNS} obtained in this approximation is unitary. For a numerical analysis without this approximation which leads to non-unitarity, please refer to appendix B.

From eq. (4.14), we extract the three mixing angles in the active sector,

$$\sin^2\theta_{13} = \frac{2\kappa_a^2}{3(1+\kappa_s^2+\kappa_a^2)}, \tag{4.15}$$

$$\sin^2\theta_{12} = \frac{1+\kappa_s^2+\kappa_a^2}{3+3\kappa_s^2+\kappa_a^2}, \tag{4.16}$$

$$\sin^2\theta_{23} = \frac{3+3\kappa_s^2+2\sqrt{3}\kappa_a+\kappa_a^2}{2(3+3\kappa_s^2+\kappa_a^2)}. \tag{4.17}$$

Eq. (4.15) and eq. (4.16) are consistent with the TM$_2$ constraint, $\sin^2\theta_{12}\cos^2\theta_{13} = \frac{1}{3}$. Using eqs. (4.13), (4.15)–(4.17), we obtain another constraint among the observables,

$$\sin^2\theta_{23} = \frac{1}{2} + \frac{3}{\sqrt{2}}\sin\theta_{13}\sin^2\theta_{12}\left(\frac{\Delta m_{21}^2}{\Delta m_{31}^2}\right)^{\frac{1}{4}}, \tag{4.18}$$

which shows the deviation from the maximal atmospheric mixing, i.e. $\sin^2\theta_{23} = \frac{1}{2}$. We also calculate the Jalskog's CP-violation parameter [69] in the active sector,

$$J = \text{Im}(U_{e2}U_{\mu3}U_{e3}^*U_{\mu2}^*) = -\frac{\kappa_s\kappa_a}{3\sqrt{3}(1+\kappa_s^2+\kappa_a^2)}. \tag{4.19}$$

Eliminating κ_s and κ_a from eq. (4.19) using eqs. (4.13), (4.15), we can express J in terms of the reactor angle and the light neutrino masses,

$$J = -\frac{1}{3\sqrt{2}}\sin\theta_{13}\sqrt{1-\frac{3}{2}\sin^2\theta_{13}-\frac{\sqrt{\Delta m_{21}^2}}{\sqrt{\Delta m_{31}^2}}}. \tag{4.20}$$

Given the three mixing angles and J in terms of the model parameters, we can obtain $\sin\delta$ using the following expression:

$$\sin\delta = J/(\sin\theta_{13}\sin\theta_{12}\sin\theta_{23}\cos^2\theta_{13}\cos\theta_{12}\cos\theta_{23}). \tag{4.21}$$

Note that the 4×4 mixing matrix is parametrised using six mixing angles (θ_{13}, θ_{12}, θ_{23}, θ_{14}, θ_{24}, θ_{34}) and three Dirac CP phases (δ_{13}, δ_{14}, δ_{24}) with the help of the parametrization mentioned in ref. [23]. However, we used the parametrisation for the 3×3 mixing matrix, eq. (1.1), to extract the mixing angles (θ_{13}, θ_{12}, θ_{23}) and the CP phase ($\delta = \delta_{13}$) given in eqs. (4.15), (4.16), (4.17), (4.21). This approximation is valid since the active-sterile mixing is quite small.

Comparing eqs. (2.10), (2.12) with eq. (4.8), it is clear that the model parameter m_s corresponds to the mass of the 4$^{\text{th}}$ mass eigenstate,

$$m_4 = m_s. \tag{4.22}$$

Using eq. (2.16), we obtain the three-component column vector R,

$$R = \sqrt{\frac{m}{2m_s}}\begin{pmatrix} 1-i(\kappa_s-\kappa_a) \\ 0 \\ 1-i(\kappa_s+\kappa_a) \end{pmatrix}. \tag{4.23}$$

– 11 –

Substituting eqs. (4.3), (4.23) in eq. (2.18) we obtain

$$U_{e4} = \frac{\sqrt{2m}}{\sqrt{3m_s}}(1 - i\kappa_s), \tag{4.24}$$

$$U_{\mu 4} = -\frac{\bar{\omega}\sqrt{m}}{\sqrt{6m_s}}(1 - i\kappa_s + \sqrt{3}\kappa_a), \tag{4.25}$$

$$U_{\tau 4} = -\frac{\omega\sqrt{m}}{\sqrt{6m_s}}(1 - i\kappa_s - \sqrt{3}\kappa_a). \tag{4.26}$$

Using eqs. (4.24), (4.25), (4.26), we can write the three active-sterile mixing angles in terms of the model parameters,

$$\sin^2\theta_{14} = \frac{2}{3}\frac{m}{m_s}(1 + \kappa_s^2), \tag{4.27}$$

$$\sin^2\theta_{24} = \frac{1}{6}\frac{m}{m_s}\frac{(1 + \kappa_s^2 + 2\sqrt{3}\kappa_a + 3\kappa_a^2)}{1 - \frac{2}{3}\frac{m}{m_s}(1 + \kappa_s^2)}, \tag{4.28}$$

$$\sin^2\theta_{34} = \frac{1}{6}\frac{m}{m_s}\frac{(1 + \kappa_s^2 - 2\sqrt{3}\kappa_a + 3\kappa_a^2)}{1 - \frac{2}{3}\frac{m}{m_s}(1 + \kappa_s^2) - \frac{1}{6}\frac{m}{m_s}(1 + \kappa_s^2 + 2\sqrt{3}\kappa_a + 3\kappa_a^2)}. \tag{4.29}$$

For the extraction of δ_{14} and δ_{24}, we need to calculate the Jarlskog-like rephasing invariants from the active-sterile sector. In this context, we refer the readers to a recent work [70], in which nine independent rephasing invariants in terms of the six mixing angles and the three Dirac phases have been evaluated in the context of the 4×4 mixing matrix. With the help of these invariants, we may extract δ_{14} and δ_{24}.

The effective neutrino mass applicable to the neutrinoless double-beta decay [71, 72] is given by

$$m_{\beta\beta} = \left| m_1 U_{e1}^2 + m_2 U_{e2}^2 + m_3 U_{e3}^2 + m_s U_{e4}^2 \right|. \tag{4.30}$$

Substituting the values of the neutrinos masses, eq. (4.13), the elements of the first row of the mixing matrix, eq. (4.14), and the expression for U_{e4}, eq. (4.24), in the above equation, we obtain

$$m_{\beta\beta} = \left| \frac{m}{3}(1 - 2\kappa_s^2 + 2\kappa_a^2 - 4i\kappa_s) \right| = \frac{m}{3}\sqrt{(1 - 2\kappa_s^2 + 2\kappa_a^2)^2 + 16\kappa_s^2}. \tag{4.31}$$

5 Phenomenology and predictions

Our model allows only four degrees of freedom in the neutrino Yukawa sector, denoted by the free parameters κ_s, κ_a, m, m_s. There are eleven independent experimentally measured quantities, $\sin^2\theta_{12}$, $\sin^2\theta_{23}$, $\sin^2\theta_{13}$, $\sin\delta$, Δm_{21}^2, Δm_{31}^2, $m_{\beta\beta}$, Δm_{41}^2, $|U_{e4}|^2$, $|U_{\mu 4}|^2$, $|U_{\tau 4}|^2$ all of which can be expressed in terms of the above mentioned four model parameters. So, it is clear that the model is extremely constrained. In this section, we calculate the model parameters using the experimental data and also make predictions. To calculate the allowed ranges of the model parameters, κ_s, κ_a, m and m_s, we utilize the observables $\sin^2\theta_{13}$, Δm_{21}^2, Δm_{31}^2 and Δm_{41}^2 whose experimental values are given in table 3. These values are obtained from the global fit data published by the nufit group [73] and the active-sterile mixing data from ref. [74].

	3σ range
$\sin^2\theta_{13}$	$0.02044 \to 0.02437$
Δm_{21}^2	$6.79 \times 10^{-5}\ \text{eV}^2 \to 8.01 \times 10^{-5}\ \text{eV}^2$
Δm_{31}^2	$2.431 \times 10^{-3}\ \text{eV}^2 \to 2.622 \times 10^{-3}\ \text{eV}^2$
Δm_{41}^2	$0.87\ \text{eV}^2 \to 2.04\ \text{eV}^2$

Table 3. The mixing observables which are used to evaluate the model parameters κ_s, κ_a, m and m_s. The 3σ ranges of $\sin^2\theta_{13}$, Δm_{21}^2 and Δm_{31}^2 are taken from ref. [73] and that of Δm_{41}^2 is taken from ref. [74].
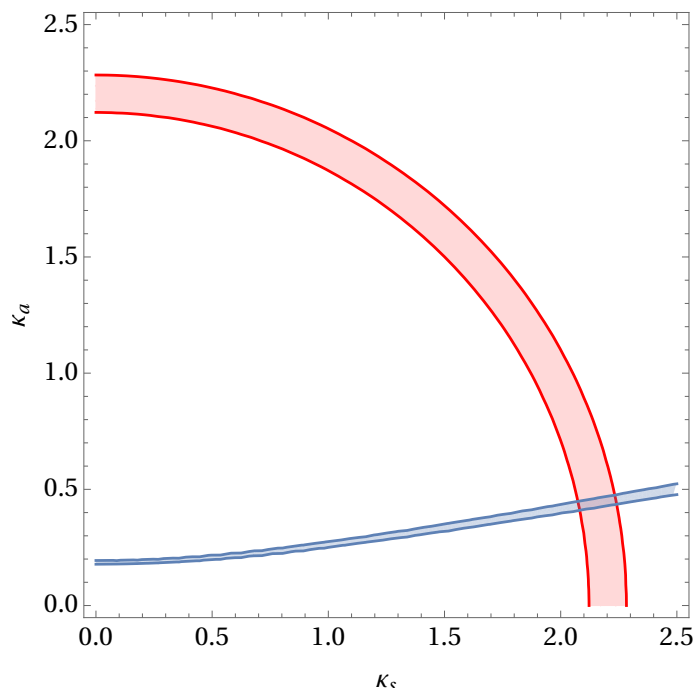
Figure 1. The parameters κ_s and κ_a constrained using the reactor mixing angle and the ratio of the mass-squared differences of the active neutrinos.

Using the expression of the reactor mixing angle given in eq. (4.15) and its range given in table 3, we obtain

$$0.02044 \leq \frac{2\kappa_a^2}{3(1 + \kappa_s^2 + \kappa_a^2)} \leq 0.02437. \tag{5.1}$$

Using eq. (4.13), we calculate the ratio of the mass-squared differences of the active neutrinos,

$$\frac{\Delta m_{31}^2}{\Delta m_{21}^2} = (1 + \kappa_s^2 + \kappa_a^2)^2. \tag{5.2}$$

Given the ranges of Δm_{21}^2 and Δm_{31}^2 (table 3), eq. (5.2) leads to

$$30.3 \leq (1 + \kappa_s^2 + \kappa_a^2)^2 \leq 38.6. \tag{5.3}$$

We use eqs. (5.1), (5.3) to constrain the parameters κ_s and κ_a. In this analysis, we chose $\sin^2\theta_{13}$ and $\frac{\Delta m_{31}^2}{\Delta m_{21}^2}$ because these are the most precisely measured observables that can
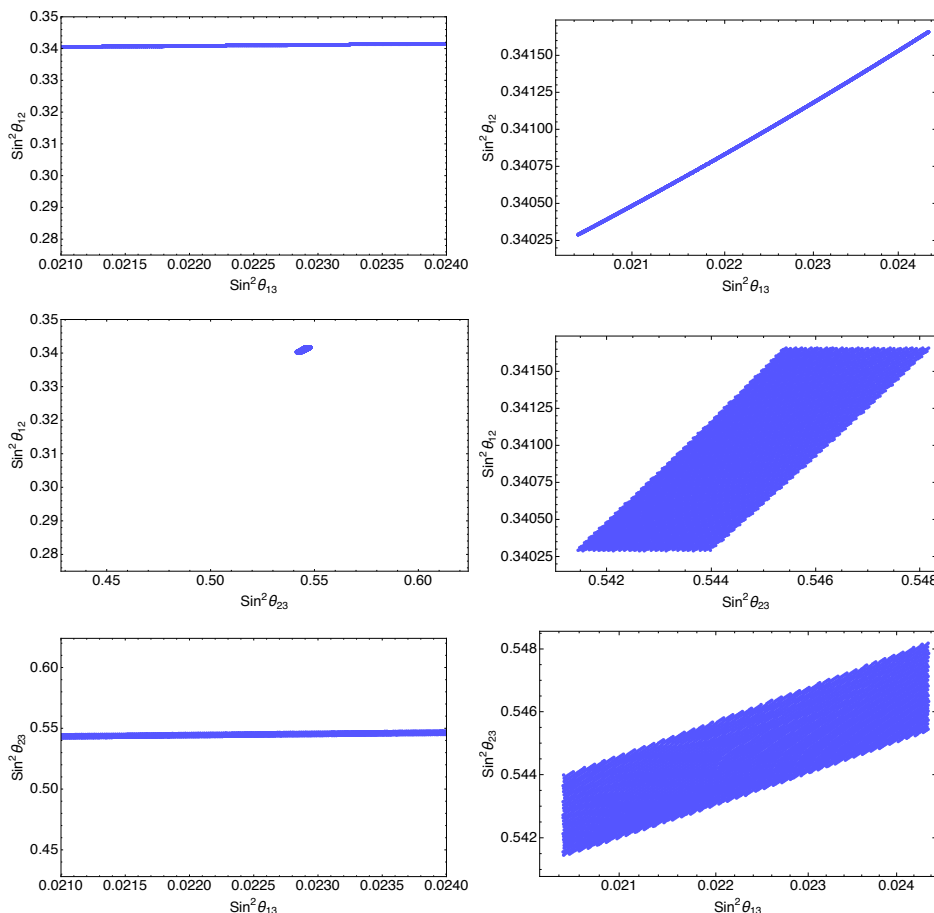
Figure 2. Correlations among the mixing angles found using equations (4.15)), (4.16 and 4.17. For an explanation please see the text. In the left panel, the predicted ranges of the observables are plotted against their entire 3σ ranges. The right panel shows the correlations among the angles which is not clearly visible in the left panel.

be used for constraining κ_s and κ_a. The results are shown in figure 1 where the blue and the red regions represent the constraints eq. (5.1) and eq. (5.3) respectively. The allowed range of κ_s and κ_a is given by the intersection of the red and the blue regions. Note that these parameters can be directly expressed in terms of the observables:

$$\kappa_s^2 = \left(1 - \frac{3}{2}\sin^2\theta_{13}\right)\frac{\sqrt{\Delta m_{31}^2}}{\sqrt{\Delta m_{21}^2}} - 1, \qquad \kappa_a^2 = \frac{3}{2}\sin^2\theta_{13}\frac{\sqrt{\Delta m_{31}^2}}{\sqrt{\Delta m_{21}^2}}. \tag{5.4}$$

The best fit values, i.e. $\sin^2\theta_{13} = 0.02237$, $\Delta m_{21}^2 = 7.39 \times 10^{-5}$ eV^2 and $\Delta m_{31}^2 = 2.528 \times 10^{-3}$ eV^2, leads to $\kappa_s = 2.16$ and $\kappa_a = 0.44$ consistent with figure 1.

Substituting this range of values in the expression of the solar mixing angle, eq. (4.16), we predict

$$0.340 \leq \sin^2\theta_{12} \leq 0.342. \tag{5.5}$$

TM$_2$ mixing fixes $|U_{e2}|^2$ to be $\frac{1}{3}$. We also have $|U_{e2}|^2 = \sin^2\theta_{12}\cos^2\theta_{13}$. Therefore, TM$_2$ scheme strongly constrains θ_{12} given the precise experimental determination of θ_{13}.

	Prediction	Experimental range
$\sin^2 \theta_{12}$	$0.340 \to 0.342$	$0.275 \to 0.350$
$\sin^2 \theta_{23}$	$0.541 \to 0.548$	$0.428 \to 0.624$
$\sin \delta$	$-0.916 \to -0.905$	$-1 \to 0.707$
$|U_{e4}|^2$	$0.021 \to 0.038$	$0.012 \to 0.047$
$|U_{\mu4}|^2$	$0.007 \to 0.013$	$0.005 \to 0.03$
$|U_{\tau4}|^2$	$0.004 \to 0.008$	< 0.16
$m_{\beta\beta}$	$0.0302 \text{ eV} \to 0.0371 \text{ eV}$	$< 0.05 \text{ eV}$

Table 4. The values of the observables predicted by the model in comparison to their experimental ranges [73, 74, 77]. $m_{\beta\beta} < 0.05$ eV is the most stringent bound from the KamLAND-Zen experiment [77].

The resulting prediction, eq. (5.5), is consistent with the 3σ experimental range $0.275 \leq \sin^2 \theta_{12} \leq 0.350$, table 4. However, a more precise determination of the solar mixing angle, for instance from reactor experiments [75, 76] can test this prediction.

Substituting the allowed range of κ_s and κ_a in the expressions of the atmospheric mixing angle, the Jarlskog invariant and the Dirac CP phase, eqs. (4.17)–(4.21), we predict

$$0.541 \leq \sin^2 \theta_{23} \leq 0.548, \tag{5.6}$$

$$-0.916 \leq \sin \delta \leq -0.905 \quad \text{with} \quad -0.0329 \leq J \leq -0.0299. \tag{5.7}$$

These predictions are also consistent with the experimental ranges, table 4. Note that the determination of the octant of θ_{23} is still an open problem experimentally. If the μ-τ reflection symmetry [78–83] is broken, we have θ_{23} either in the first or the second octant. The model predicts it to be in the second octant.

In figure 2, we show the correlations among the mixing angles resulting from the model. The top panel of the figure shows the TM$_2$ constraint between the solar and reactor mixing angles, $\sin^2 \theta_{12} \cos^2 \theta_{13} = \frac{1}{3}$. For small θ_{13}, we obtain a linear relationship, $\sin^2 \theta_{12} \simeq \frac{1}{3}(1 + \sin^2 \theta_{13})$. The mild positive correlations of the atmospheric angle with the solar and the reactor angles shown in the middle and the bottom panels respectively are nothing but the result of the constraint among these quantities given in eq. (4.18). We also note that the deviation from maximal atmospheric mixing shown in these plots (0.041-0.048) is consistent with the deviation obtained in eq. (4.18).

The global fit [73] of oscillation data gives hints for CP violation. Even though the measurement is not precise, $135° \leq \delta \leq 366°$, it favours a relatively large negative value for $\sin \delta$. Our prediction, eq. (5.7), supports this scenario. In figure 3, we have shown the predictions for $\sin^2 \theta_{23}$ and $\sin \delta$.

Under the MES scheme, the mass of the lightest neutrino, m_1, vanishes.[6] Therefore, the experimental ranges of Δm_{21}^2 and Δm_{31}^2, table 3, leads to the prediction,

$$8.24 \times 10^{-3} \text{ eV} \leq m_2 \leq 8.95 \times 10^{-3} \text{ eV}, \quad 4.93 \times 10^{-2} \text{ eV} \leq m_3 \leq 5.12 \times 10^{-2} \text{ eV}. \tag{5.8}$$

---

[6]The higher-order corrections in the MES framework will generate non-zero mass for m_1, albeit tiny. Here we ignore this mass. In appendix B, we estimate it to be of the order of 10^{-5} eV.
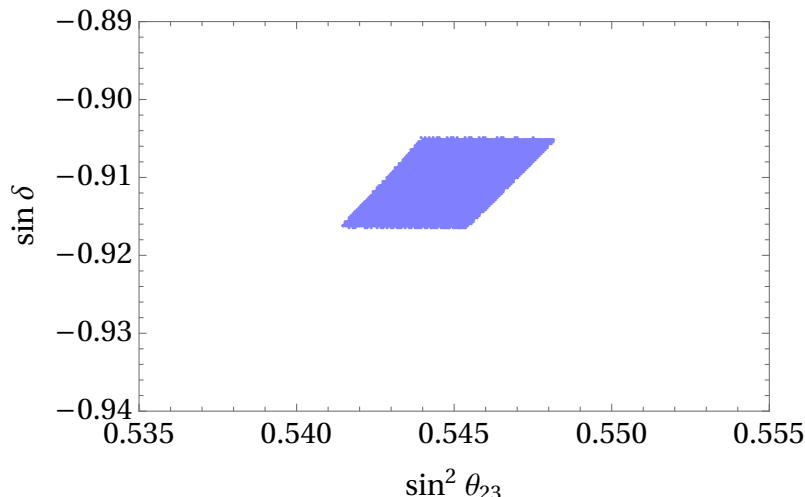
Figure 3. The predicted ranges of $\sin^2\theta_{23}$ and $\sin\delta$ as constrained by the parameters κ_s and κ_a.

(a) $|U_{e4}|^2$ vs m_s

(b) $|U_{\mu4}|^2$ vs m_s
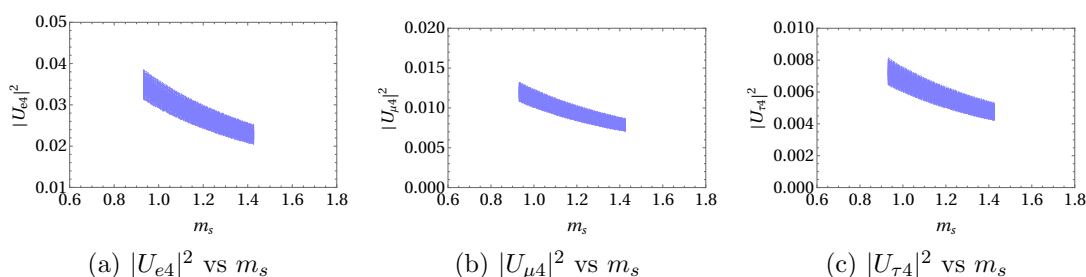
(c) $|U_{\tau4}|^2$ vs m_s

Figure 4. The active-sterile mixing observables predicted by the model plotted against m_s. These curves show the inverse relationship between the moduli-squared values of the active-sterile mixing elements and the sterile neutrino mass as can be inferred from eqs. (4.24)–(4.26).

The model parameter m corresponds to the neutrino mass m_2, so its allowed range is the same as that of m_2 given above. Using the range of Δm_{41}^2 from table 3, we obtain,

$$0.93 \text{ eV} \leq m_4 \leq 1.42 \text{ eV}, \tag{5.9}$$

which also corresponds to the range of the model parameter, m_s, eq. (4.22).

The active-sterile mixing observables, eqs. (4.24)–(4.26), depend on all the four model parameters, κ_s, κ_a, m, and m_s. By varying these parameters within their respective ranges we predict the values of these observables, i.e. $|U_{e4}|^2$, $|U_{\mu4}|^2$ and $|U_{\tau4}|^2$, table 4. These predictions are well within their corresponding experimental ranges. In figure 4, we have plotted them against the parameter, m_s.

Substituting the allowed ranges of κ_s, κ_a, m, and m_s in eq. (4.31), we predict the value of the neutrinoless double-beta decay mass, table 4, which is also shown in figure 5. This range is quite narrow because the model strongly constrains the first row of the mixing matrix through the parameters κ_s and κ_a, which effectively constrains the Majorana phases as well.

Cosmological observations set upper bounds to the sum of the neutrino masses for three generations of neutrinos, $\Sigma m_i = m_1 + m_2 + m_3$. However, in the presence of the
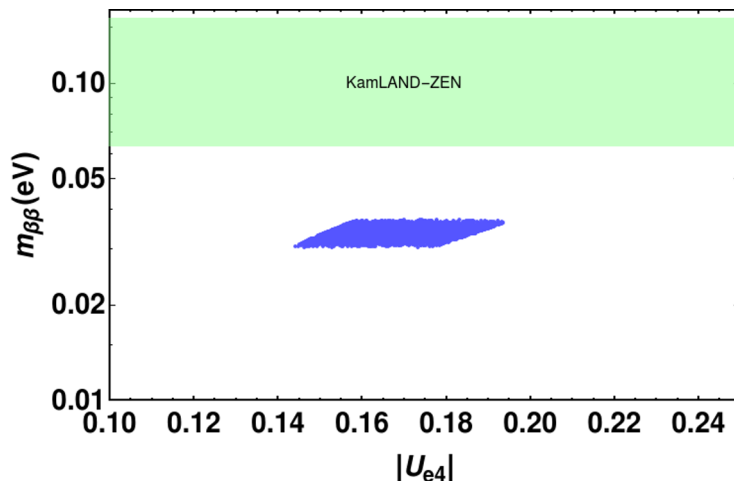
Figure 5. The prediction of the effective neutrino mass, $m_{\beta\beta}$, in relation to the active-sterile mixing strength.

sterile neutrino, the bound gets affected. At the same time, some recent cosmological models offer an explanation in favour of the existence of the sterile neutrino via the so-called secret interactions. The broken $U(1)_s$ gauge symmetry in our model will lead to a massive gauge boson which can mediate such an interaction. For a detailed discussion about the cosmological implications of sterile neutrinos having secret interactions, please see the references [66–68].

6 Discussion and conclusion

In this paper, we construct the leptonic mass matrices in terms of the VEVs of a set of flavon fields transforming under the discrete symmetry group $A_4 \times C_4 \times C_6 \times C_2$ and the VEVs of the SM Higgs and a sterile sector Higgs. In the charged-lepton sector, we obtain a non-diagonal mass matrix. In the neutrino sector, we use the MES formula, eq. (2.11), to construct the effective 3×3 seesaw mass matrix. The unitary matrices U_L and U_ν diagonalise the charged-lepton and the neutrino mass matrices respectively. Their product determines the mixing in the active sector, i.e. $U_{\text{PMNS}} \simeq U_L U_\nu$, eq. (2.19). In our model, the unitary contribution from the charged-lepton sector (U_L) has a 3×3 trimaximal form, eq. (4.3). On the other hand, the contribution from the active neutrino sector (U_ν) has the form which corresponds to the second flavour eigenstate being equal to the second mass eigenstate as evident from the off-diagonal zeros in U_ν, eq. (4.11). Consequently, the second column of U_L is preserved in the product $U_L U_\nu$ and as a result, we obtain the TM$_2$ mixing.

U_ν obtained in the model contains two parameters κ_s and κ_a. These parameters correspond to the symmetric and the antisymmetric parts of the neutrino mass matrix, M_D, which in turn originate from the symmetric and the antisymmetric parts of the tensor product of triplets of A_4. If κ_a vanishes, U_ν becomes bimaximal, i.e.

$$\kappa_a \to 0 \implies U_\nu \to \begin{pmatrix} \frac{1}{\sqrt{2}} & 0 & \frac{-1}{\sqrt{2}} \\ 0 & 1 & 0 \\ \frac{1}{\sqrt{2}} & 0 & \frac{1}{\sqrt{2}} \end{pmatrix}, \tag{6.1}$$

which will lead to tribimaximal (TBM) mixing. The observation of non-zero reactor angle has ruled out TBM. Hence, the parameter κ_a plays the vital role of generating the non-zero reactor angle in the model. This role has been emphasized in ref. [84].

We obtain CP violation even though all the free parameters in the model are real. The charged-lepton mass matrix, M_l, eq. (4.1), and the neutrino mass matrix, M_D, eq. (4.5), turn out to be complex on account of the complex VEVs $\langle \phi_l \rangle$ and $\langle \phi \rangle$ respectively. Hence CP is broken spontaneously in the model. Since M_l and M_D are complex, the corresponding diagonalising matrices U_L and U_ν also become complex and they generate the complex mixing matrix, $U_{\mathrm{PMNS}} \simeq U_L U_\nu$. It can be shown that if U_ν were real, the resulting mixing matrix $U_L U_\nu$ would be symmetric under μ-τ reflection implying $\theta_{23} = \frac{\pi}{4}$. In such a scenario, despite U_ν being real, CP would be maximally broken ($\delta = \pm\frac{\pi}{2}$) because of the complex contribution from the charged-lepton sector (U_L) alone. Our model, with U_ν also being complex, breaks μ-τ reflection symmetry and we obtain $\theta_{23} \neq \frac{\pi}{4}$. The complex U_ν also shifts δ away from its maximal value, i.e. $\delta \neq \pm\frac{\pi}{2}$. Therefore, the origin of the non-maximal values of the atmospheric mixing as well as the CP phase is the complex VEV, $\langle \phi \rangle$.

LSND and MiniBooNE observations suggest the existence of sterile neutrinos. The observed active-sterile mixing ($|U_{e4}|^2$, $|U_{\mu4}|^2$) is found to be of the order of $\frac{\sqrt{\Delta m_{21}^2}}{\sqrt{\Delta m_{41}^2}}$. The Minimal Extended Seesaw provides a natural framework to achieve this relationship. It is in this context that we built the model to explain both the active and the sterile mixing observables. In the model, these observables are given in terms of four parameters, κ_s, κ_a, m and m_s. We use the experimental ranges of the reactor mixing angle, $\sin^2\theta_{13}$, and the mass-squared differences, Δm_{21}^2 and Δm_{31}^2, to extract the allowed values of κ_s, κ_a and m, as we obtain $m_2 < m_3$ corresponding to normal hierarchy. The extracted values of κ_s and κ_a are used to predict θ_{23} and δ. These predictions can be tested when these observables are measured more precisely in future oscillation experiments. The model parameter, m_s, corresponds to the sterile neutrino mass and is determined by the active-sterile mass-squared difference, Δm_{41}^2. The three model parameters, κ_s, κ_a and m (constrained using $\sin^2\theta_{13}$, Δm_{21}^2 and Δm_{31}^2), as well as the fourth parameter, m_s (constrained using Δm_{41}^2), are used to evaluate the active-sterile mixing. We find that these values are consistent with the experimental results. We also obtain strong constraints on the range of the effective mass governing the neutrinoless double-beta decay.

A   Uniquely defining the flavon VEVs

The model contains the flavon multiplets, ϕ_l, η, ϕ, ϕ_s and η_ν. The alignments of their VEVs in the flavour space play a crucial role in determining the model's phenomenology. In this appendix, we provide justifications for these alignments by uniquely defining them using symmetries.

The flavon ϕ_l couples in the charged-lepton sector. Consider the alignment $\langle \phi_l \rangle \propto (1, \bar{\omega}, \omega)^T$, eq. (3.9). This VEV is invariant under the following group action:

$$\omega T \langle \phi_l \rangle = \langle \phi_l \rangle, \tag{A.1}$$

where ω and T are elements of C_3 and A_4 respectively under which ϕ_l transforms. In other words, ωT generates the residual symmetry of $\langle \phi_l \rangle$ and this symmetry uniquely defines $\langle \phi_l \rangle$ (up to multiplication with a constant[7]). A triplet flavon whose VEV is defined by the residual symmetry, eq. (A.1), was recently utilised in the construction of the charged-lepton mass matrix in ref. [85].

The singlet η and the triplet ϕ couple in the neutrino Dirac sector. The VEV of the singlet, eq. (3.10), is assumed to be real. This can be ensured by assuming the residual symmetry under conjugation,

$$\langle \eta \rangle^* = \langle \eta \rangle. \tag{A.2}$$

The VEV $\langle \phi \rangle \propto (0, -i, 0)^T$, eq. (3.11), is uniquely defined using the residual symmetries,

$$T^2 ST \langle \phi \rangle = \langle \phi \rangle, \quad -1 \langle \phi \rangle^* = \langle \phi \rangle. \tag{A.3}$$

These symmetries ensure that the first and the third components of $\langle \phi \rangle$ vanish and the phase of the second component is $-i$. Note that the constant of proportionality in the VEV, i.e. v_ϕ in eq. (3.11), is real.

The triplet ϕ_s couples in the sterile sector. Its VEV, $\langle \phi_s \rangle \propto (1, 0, 1)^T$, eq. (3.12), has the following residual symmetries:

$$-1 \, T^2 ST \langle \phi_s \rangle = \langle \phi_s \rangle, \quad \langle \phi_s \rangle^* = \langle \phi_s \rangle. \tag{A.4}$$

The VEV of the A_4 triplet in the form $\propto (1, 0, 1)^T$ has been widely used in the literature [86–88]. This alignment can be uniquely obtained from the symmetric tensor product involving the alignments $(0, 1, 0)^T$ and $(1, 1, 1)^T$,[8]

$$\left((0, 1, 0)^T, (1, 1, 1)^T \right)_{\mathbf{3}_s} \propto (1, 0, 1)^T. \tag{A.5}$$

The VEV of the singlet η_ν can be trivially assigned any complex constant since its phase has no effect on the model's phenomenology.

Here we have assumed that various flavon VEVs have distinct residual symmetries. It is interesting to note that if all the VEVs are taken together, none of these symmetries survive. A comprehensive study of the origin of the VEVs requires the construction of the flavon potential. If different irreducible multiplets are decoupled in the potential, then it can lead to the corresponding VEVs having separate residual symmetries. The construction of a potential with an inbuilt mechanism to ensure the decoupling of the irreducible multiplets is beyond the scope of this work. However, we assume that our VEVs are generated from such a potential.

B   Numerical verification of approximations

In this appendix, we construct the charged-lepton and the neutrino mass matrices using a representative set of model parameters and numerically extract the masses and the mixing

---

[7]This constant, i.e. v_l in eq. (3.9), can be complex in general. Note that v_l being complex does not alter the phenomenology of the charged-lepton sector.

[8]The alignment $(1, 1, 1)^T$ can be uniquely defined by the residual symmetry, $T(1, 1, 1)^T = (1, 1, 1)^T$.

observables without employing approximations. Thus we verify the correctness of the various results obtained in the main body of the paper. In our calculations, we use

$$\Lambda = 10^{13}, \quad v_x = 10^{10}, \tag{B.1}$$

where v_x represents v_l, v_η, v_ϕ, v_s and v_ν. All mass units are given in GeV, unless otherwise specified. The SM Higgs and the sterile Higgs are given the following VEVs,

$$v = 176, \tag{B.2}$$

$$v' = 2000. \tag{B.3}$$

Substituting eqs. (B.1), (B.2) in eq. (4.1), we obtain the charged-lepton mass matrix in the form,

$$M_l = 176 \times 10^{-6} \begin{pmatrix} (1.7 - i0.9)Y_e \ 0 \ 0 \\ (0.8 - i1.5)Y_e \ 0 \ 0 \\ (1.7 - i0.9)Y_e \ 0 \ 0 \end{pmatrix} + 176 \times 10^{-3} \begin{pmatrix} 0 \ Y_\mu \ Y_\tau \\ 0 \ \omega Y_\mu \ \bar{\omega} Y_\tau \\ 0 \ \bar{\omega} Y_\mu \ \omega Y_\tau \end{pmatrix}. \tag{B.4}$$

Since several higher-order flavon triplets contribute in the construction of the electron mass term, there will be a corresponding set of Yukawa-like free parameters. We assign random real numbers to these parameters resulting in the first column of M_l, eq. (B.4).[9] For convenience, we have introduced a parameter Y_e in this column. Diagonalising M_l using the unitary matrices U_L and U_R, eq. (4.2), produces the charged-lepton masses. Their experimental values ($m_\tau = 1777\,\text{MeV}$, $m_\mu = 106\,\text{MeV}$ and $m_e = 0.511\,\text{MeV}$) are obtained with the substitution,

$$Y_\tau = \frac{1}{\sqrt{3}} \frac{1}{176} 1777 = 5.83, \quad Y_\mu = \frac{1}{\sqrt{3}} \frac{1}{176} 106 = 0.348, \quad Y_e = 0.942. \tag{B.5}$$

These coupling constants are of the order of one as we expect. The corresponding diagonalising matrices are

$$U_L = \begin{pmatrix} 0.577 & 0.577 & 0.577 \\ 0.577 & -0.289 - i0.500 & -0.289 + i0.500 \\ 0.577 & -0.289 + i0.500 & -0.289 - i0.500 \end{pmatrix}, \tag{B.6}$$

$$U_R = \begin{pmatrix} 0.786 - i0.618 & 0.001 + i0.001 & 0.000 \\ i0.001 & 1.000 & 0.000 \\ 0.000 & 0.000 & 1.000 \end{pmatrix}. \tag{B.7}$$

We find that the above calculation of U_L is consistent with the expression given in eq. (4.3) within a deviation of the order of $\frac{v_x^2}{\Lambda^2}$.

To construct the neutrino mass matrices, we make the following assignments:

$$Y_\eta = 1.67, \quad Y_{\phi s} = 3.59, \quad Y_{\phi a} = 0.80, \quad Y_s = 1.23, \quad Y_\nu = 1.00. \tag{B.8}$$

---

[9]The exact values of these numbers are irrelevant in an order-of-magnitude calculation.

Substituting eqs. (B.1)–(B.3), (B.8) in eqs. (4.5)–(4.7), we obtain

$$M_D = \begin{pmatrix} 0.294 & 0 & -i0.491 \\ 0 & 0.294 & 0 \\ -i0.773 & 0 & 0.294 \end{pmatrix}, \quad M_s = (2.46, 0, 2.46), \quad M_R = \text{diag}(1,1,1)10^{10}.$$
(B.9)

We also introduce mass matrices involving $\bar{\nu}_L \nu_L^c$, $\bar{\nu}_L \nu_s$ and $\bar{\nu}_s^c \nu_s$, which are highly suppressed as described at the end of section 3,

$$\bar{\nu}_L \nu_L^c: \quad M_1 = \begin{pmatrix} 1.24 & -2.32 - i4.02 & -1.39 + i4.02 \\ -2.32 - i4.02 & 1.24 & 4.65 \\ -1.39 + i4.02 & 4.65 & 1.24 \end{pmatrix} 10^{-15},$$
(B.10)

$$\bar{\nu}_L \nu_s: \quad M_2 = \begin{pmatrix} 2.11 - i1.41 \\ 0 \\ 2.11 + i2.82 \end{pmatrix} 10^{-14}, \quad \bar{\nu}_s^c \nu_s: \quad M_3 = \begin{pmatrix} 2.80 \end{pmatrix} 10^{-13}.$$
(B.11)

Here also, the matrices have been populated with a random choice of Yukawa-like couplings corresponding to the higher-order terms. In terms of eqs. (B.9)–(B.11), we construct the neutrino mass matrix in the '$\nu = (\nu_L, \nu_s^c, \nu_R^c)$'-basis:

$$\bar{\nu}\nu^c: \quad M_\nu^{7\times7} = \begin{pmatrix} M_1 & M_2 & M_D \\ M_2^T & M_3 & M_s \\ M_D^T & M_s^T & M_R \end{pmatrix}.$$
(B.12)

This matrix is diagonalised to obtain the neutrino masses,

$$U_\nu^{7\times7\dagger} M_\nu^{7\times7} U_\nu^{7\times7*} =$$
$$\text{diag}\left(1.4 \times 10^{-14}, 8.6 \times 10^{-12}, 5.0 \times 10^{-11}, 1.3 \times 10^{-9}, 1.0 \times 10^{10}, 1.0 \times 10^{10}, 1.0 \times 10^{10}\right),$$
(B.13)

where

$$U_\nu^{7\times7} = \begin{pmatrix} U_\nu^{4\times4} & \mathcal{O}(10^{-10}) \\ \mathcal{O}(10^{-10}) & U_\nu^{\text{heavy}} \end{pmatrix}.$$
(B.14)

The structure of U_ν^{heavy} depends on the higher-order corrections to M_R which break the degeneracy of the heavy neutrino masses. These corrections are of no significance to the present work. We note that the mass acquired by the lightest neutrino is of the order of $M_2 = \mathcal{O}(10^{-14})$.

The 4×4 light-neutrino mixing matrix is obtained as

$$U = \begin{pmatrix} U_L & 0 \\ 0 & 1 \end{pmatrix} U_\nu^{4\times4} = \begin{pmatrix} -0.332 + i0.713 & 0.571 + i0.086 & -0.059 + i0.137 & 0.067 - i0.146 \\ -0.323 + i0.154 & -0.212 - i0.537 & -0.438 - i0.581 & 0.096 + i0.017 \\ 0.157 + i0.441 & -0.359 + i0.452 & 0.373 - i0.551 & -0.060 - i0.039 \\ 0.185 & 0.000 & 0.079 & 0.980 \end{pmatrix},$$
(B.15)

This matrix is consistent with the results we obtained using the seesaw approximations.

References

[1] P. Minkowski, $\mu \to e\gamma$ *at a rate of one out of* 10^9 *muon decays?*, *Phys. Lett. B* **67** (1977) 421 [INSPIRE].

[2] M. Gell-Mann, P. Ramond and R. Slansky, *Complex spinors and unified theories*, *Conf. Proc. C* **790927** (1979) 315 [arXiv:1306.4669] [INSPIRE].

[3] T. Yanagida, *Horizontal gauge symmetry and masses of neutrinos*, talk given at the *Workshop on Unified Theory and Baryon Number in the Universe*, January 13–14, Tsukuba, Japan (1979).

[4] R.N. Mohapatra and G. Senjanović, *Neutrino mass and spontaneous parity nonconservation*, *Phys. Rev. Lett.* **44** (1980) 912 [INSPIRE].

[5] PLANCK collaboration, *Planck 2018 results. VI. Cosmological parameters*, arXiv:1807.06209 [INSPIRE].

[6] KATRIN collaboration, *First operation of the KATRIN experiment with tritium*, *Eur. Phys. J. C* **80** (2020) 264 [arXiv:1909.06069] [INSPIRE].

[7] LSND collaboration, *Evidence for anti-muon-neutrino → anti-electron-neutrino oscillations from the LSND experiment at LAMPF*, *Phys. Rev. Lett.* **77** (1996) 3082 [nucl-ex/9605003] [INSPIRE].

[8] LSND collaboration, *Evidence for neutrino oscillations from the observation of* $\bar{\nu}_e$ *appearance in a* $\bar{\nu}_\mu$ *??beam*, *Phys. Rev. D* **64** (2001) 112007 [hep-ex/0104049] [INSPIRE].

[9] MINIBOONE collaboration, *A combined* $\nu_\mu \to \nu_e$ *and* $\bar{\nu}_\mu \to \bar{\nu}_e$ *oscillation analysis of the MiniBooNE excesses*, 7, 2012 [arXiv:1207.4809] [INSPIRE].

[10] MINIBOONE collaboration, *Significant excess of electronlike events in the MiniBooNE short-baseline neutrino experiment*, *Phys. Rev. Lett.* **121** (2018) 221801 [arXiv:1805.12028] [INSPIRE].

[11] G. Mention et al., *The reactor antineutrino anomaly*, *Phys. Rev. D* **83** (2011) 073006 [arXiv:1101.2755] [INSPIRE].

[12] T. Mueller et al., *Improved predictions of reactor antineutrino spectra*, *Phys. Rev. C* **83** (2011) 054615 [arXiv:1101.2663] [INSPIRE].

[13] P. Huber, *On the determination of anti-neutrino spectra from nuclear reactors*, *Phys. Rev. C* **84** (2011) 024617 [*Erratum ibid.* **85** (2012) 029901] [arXiv:1106.0687] [INSPIRE].

[14] M. Dentler et al., *Updated global analysis of neutrino oscillations in the presence of eV-scale sterile neutrinos*, *JHEP* **08** (2018) 010 [arXiv:1803.10661] [INSPIRE].

[15] J.N. Abdurashitov et al., *Measurement of the response of a Ga solar neutrino experiment to neutrinos from an Ar-37 source*, *Phys. Rev. C* **73** (2006) 045805 [nucl-ex/0512041] [INSPIRE].

[16] C. Giunti and M. Laveder, *Statistical significance of the gallium anomaly*, *Phys. Rev. C* **83** (2011) 065504 [arXiv:1006.3244] [INSPIRE].

[17] J. Kostensalo, J. Suhonen, C. Giunti and P.C. Srivastava, *The gallium anomaly revisited*, *Phys. Lett. B* **795** (2019) 542 [arXiv:1906.10980] [INSPIRE].

[18] S. Goswami, *Accelerator, reactor, solar and atmospheric neutrino oscillation: beyond three generations*, *Phys. Rev. D* **55** (1997) 2931 [hep-ph/9507212] [INSPIRE].

[19] J. Kopp, M. Maltoni and T. Schwetz, *Are there sterile neutrinos at the eV scale?*, *Phys. Rev. Lett.* **107** (2011) 091801 [arXiv:1103.4570] [INSPIRE].

[20] J.M. Conrad, C.M. Ignarra, G. Karagiorgi, M.H. Shaevitz and J. Spitz, *Sterile neutrino fits to short baseline neutrino oscillation measurements*, *Adv. High Energy Phys.* **2013** (2013) 163897 [arXiv:1207.4765] [INSPIRE].

[21] C. Giunti and M. Laveder, $3 + 1$ *and* $3 + 2$ *sterile neutrino fits*, *Phys. Rev. D* **84** (2011) 073008 [arXiv:1107.1452] [INSPIRE].

[22] M. Maltoni, T. Schwetz, M.A. Tortola and J.W.F. Valle, *Constraining neutrino oscillation parameters with current solar and atmospheric data*, *Phys. Rev. D* **67** (2003) 013011 [hep-ph/0207227] [INSPIRE].

[23] J. Barry, W. Rodejohann and H. Zhang, *Light sterile neutrinos: models and phenomenology*, *JHEP* **07** (2011) 091 [arXiv:1105.3911] [INSPIRE].

[24] H. Zhang, *Light sterile neutrino in the minimal extended seesaw*, *Phys. Lett. B* **714** (2012) 262 [arXiv:1110.6838] [INSPIRE].

[25] S.F. King, *Models of neutrino mass, mixing and CP-violation*, *J. Phys. G* **42** (2015) 123001 [arXiv:1510.02091] [INSPIRE].

[26] G. Altarelli and F. Feruglio, *Discrete flavor symmetries and models of neutrino mixing*, *Rev. Mod. Phys.* **82** (2010) 2701 [arXiv:1002.0211] [INSPIRE].

[27] A.Y. Smirnov, *Discrete symmetries and models of flavor mixing*, *J. Phys. Conf. Ser.* **335** (2011) 012006 [arXiv:1103.3461] [INSPIRE].

[28] S.F. King and C. Luhn, *Neutrino mass and mixing with discrete symmetry*, *Rept. Prog. Phys.* **76** (2013) 056201 [arXiv:1301.1340] [INSPIRE].

[29] P.F. Harrison, D.H. Perkins and W.G. Scott, *A redetermination of the neutrino mass squared difference in tri-maximal mixing with terrestrial matter effects*, *Phys. Lett. B* **458** (1999) 79 [hep-ph/9904297] [INSPIRE].

[30] P.F. Harrison, D.H. Perkins and W.G. Scott, *Tri-bimaximal mixing and the neutrino oscillation data*, *Phys. Lett. B* **530** (2002) 167 [hep-ph/0202074] [INSPIRE].

[31] P.F. Harrison and W.G. Scott, *Permutation symmetry, tri-bimaximal neutrino mixing and the S3 group characters*, *Phys. Lett. B* **557** (2003) 76 [hep-ph/0302025] [INSPIRE].

[32] G. Altarelli and F. Feruglio, *Tri-bimaximal neutrino mixing, A_4 and the modular symmetry*, *Nucl. Phys. B* **741** (2006) 215 [hep-ph/0512103] [INSPIRE].

[33] E. Ma, A_4 *symmetry and neutrinos with very different masses*, *Phys. Rev. D* **70** (2004) 031901R.

[34] E. Ma, *Aspects of the tetrahedral neutrino mass matrix*, *Phys. Rev. D* **72** (2005) 037301 [hep-ph/0505209] [INSPIRE].

[35] A. Zee, *Obtaining the neutrino mixing matrix with the tetrahedral group*, *Phys. Lett. B* **630** (2005) 58 [hep-ph/0508278] [INSPIRE].

[36] RENO collaboration, *Observation of reactor electron antineutrino disappearance in the RENO experiment*, *Phys. Rev. Lett.* **108** (2012) 191802 [`arXiv:1204.0626`] [ɪɴSPIRE].

[37] DOUBLE CHOOZ collaboration, *Indication of reactor $\bar{\nu}_e$ disappearance in the Double CHOOZ experiment*, *Phys. Rev. Lett.* **108** (2012) 131801 [`arXiv:1112.6353`] [ɪɴSPIRE].

[38] DAYA BAY collaboration, *Measurement of electron antineutrino oscillation based on 1230 days of operation of the Daya Bay experiment*, *Phys. Rev. D* **95** (2017) 072006 [`arXiv:1610.04802`] [ɪɴSPIRE].

[39] S.F. King and C. Luhn, *Trimaximal neutrino mixing from vacuum alignment in A_4 and S_4 models*, *JHEP* **09** (2011) 042 [`arXiv:1107.5332`] [ɪɴSPIRE].

[40] S. Antusch, S.F. King, C. Luhn and M. Spinrath, *Trimaximal mixing with predicted θ_{13} from a new type of constrained sequential dominance*, *Nucl. Phys. B* **856** (2012) 328 [`arXiv:1108.4278`] [ɪɴSPIRE].

[41] S.F. King and C. Luhn, *A4 models of tri-bimaximal-reactor mixing*, *JHEP* **03** (2012) 036 [`arXiv:1112.1959`] [ɪɴSPIRE].

[42] S. Gupta, A.S. Joshipura and K.M. Patel, *Minimal extension of tri-bimaximal mixing and generalized $Z_2 \times Z_2$ symmetries*, *Phys. Rev. D* **85** (2012) 031903 [`arXiv:1112.6113`] [ɪɴSPIRE].

[43] Z.-z. Xing, *A shift from democratic to tri-bimaximal neutrino mixing with relatively large θ_{13}*, *Phys. Lett. B* **696** (2011) 232 [`arXiv:1011.2954`] [ɪɴSPIRE].

[44] P.F. Harrison, R. Krishnan and W.G. Scott, *Deviations from tribimaximal neutrino mixing using a model with $\Delta(27)$ symmetry*, *Int. J. Mod. Phys. A* **29** (2014) 1450095 [`arXiv:1406.2025`] [ɪɴSPIRE].

[45] A. Merle, S. Morisi and W. Winter, *Common origin of reactor and sterile neutrino mixing*, *JHEP* **07** (2014) 039 [`arXiv:1402.6332`] [ɪɴSPIRE].

[46] N. Nath, M. Ghosh, S. Goswami and S. Gupta, *Phenomenological study of extended seesaw model for light sterile neutrino*, *JHEP* **03** (2017) 075 [`arXiv:1610.09090`] [ɪɴSPIRE].

[47] P. Das, A. Mukherjee and M.K. Das, *Active and sterile neutrino phenomenology with A_4 based minimal extended seesaw*, *Nucl. Phys. B* **941** (2019) 755 [`arXiv:1805.09231`] [ɪɴSPIRE].

[48] N. Sarma, K. Bora and D. Borah, *Compatibility of A_4 flavour symmetric minimal extended seesaw with $(3 + 1)$ neutrino data*, *Eur. Phys. J. C* **79** (2019) 129 [`arXiv:1810.05826`] [ɪɴSPIRE].

[49] P.S. Bhupal Dev and A. Pilaftsis, *Light and superlight sterile neutrinos in the minimal radiative inverse seesaw model*, *Phys. Rev. D* **87** (2013) 053007 [`arXiv:1212.3808`] [ɪɴSPIRE].

[50] Z.-z. Xing, H. Zhang and S. Zhou, *Nearly tri-bimaximal neutrino mixing and CP-violation from μ-τ symmetry breaking*, *Phys. Lett. B* **641** (2006) 189 [`hep-ph/0607091`] [ɪɴSPIRE].

[51] C.H. Albright and W. Rodejohann, *Comparing trimaximal mixing and its variants with deviations from tri-bimaximal mixing*, *Eur. Phys. J. C* **62** (2009) 599 [`arXiv:0812.0436`] [ɪɴSPIRE].

[52] C.H. Albright, A. Dueck and W. Rodejohann, *Possible alternatives to tri-bimaximal mixing*, *Eur. Phys. J. C* **70** (2010) 1099 [`arXiv:1004.2798`] [ɪɴSPIRE].

[53] S.-F. Ge, D.A. Dicus and W.W. Repko, *Residual symmetries for neutrino mixing with a large θ_{13} and nearly maximal δ_D*, *Phys. Rev. Lett.* **108** (2012) 041801 [arXiv:1108.0964] [INSPIRE].

[54] R. Krishnan, P.F. Harrison and W.G. Scott, *Simplest neutrino mixing from S_4 symmetry*, *JHEP* **04** (2013) 087 [arXiv:1211.2000] [INSPIRE].

[55] R. Krishnan, *A model for large Θ_{13} constructed using the eigenvectors of the S_4 rotation matrices*, *J. Phys. Conf. Ser.* **447** (2013) 012043 [arXiv:1211.3364] [INSPIRE].

[56] V.V. Vien, A.E. Cárcamo Hernández and H.N. Long, *The $\Delta(27)$ flavor 3-3-1 model with neutral leptons*, *Nucl. Phys. B* **913** (2016) 792 [arXiv:1601.03300] [INSPIRE].

[57] R. Krishnan, P.F. Harrison and W.G. Scott, *Fully constrained Majorana neutrino mass matrices using $\Sigma(72 \times 3)$*, *Eur. Phys. J. C* **78** (2018) 74 [arXiv:1801.10197] [INSPIRE].

[58] R. Krishnan, *Fully Constrained Mass Matrix: Can Symmetries alone determine the Flavon Vacuum Alignments?*, *Phys. Rev. D* **101** (2020) 075004 [arXiv:1901.01205] [INSPIRE].

[59] E. Ma and G. Rajasekaran, *Softly broken A_4 symmetry for nearly degenerate neutrino masses*, *Phys. Rev. D* **64** (2001) 113012 [hep-ph/0106291] [INSPIRE].

[60] K.S. Babu, E. Ma and J.W.F. Valle, *Underlying A_4 symmetry for the neutrino mass matrix and the quark mixing matrix*, *Phys. Lett. B* **552** (2003) 207 [hep-ph/0206292] [INSPIRE].

[61] Y. Shimizu, M. Tanimoto and A. Watanabe, *Breaking tri-bimaximal mixing and large θ_{13}*, *Prog. Theor. Phys.* **126** (2011) 81 [arXiv:1105.2929] [INSPIRE].

[62] H. Ishimori, T. Kobayashi, H. Ohki, Y. Shimizu, H. Okada and M. Tanimoto, *Non-abelian discrete symmetries in particle physics*, *Prog. Theor. Phys. Suppl.* **183** (2010) 1 [arXiv:1003.3552] [INSPIRE].

[63] W. Grimus and P.O. Ludl, *Finite flavour groups of fermions*, *J. Phys. A* **45** (2012) 233001 [arXiv:1110.6376] [INSPIRE].

[64] S.F. King and C. Luhn, *Neutrino mass and mixing with discrete symmetry*, *Rep. Prog. Phys.* **76** (2013) 056201.

[65] G. Altarelli and F. Feruglio, *Discrete flavor symmetries and models of neutrino mixing*, *Rev. Mod. Phys.* **82** (2010) 2701 [arXiv:1002.0211] [INSPIRE].

[66] B. Dasgupta and J. Kopp, *Cosmologically safe eV-scale sterile neutrinos and improved dark matter structure*, *Phys. Rev. Lett.* **112** (2014) 031803 [arXiv:1310.6337] [INSPIRE].

[67] X. Chu, B. Dasgupta, M. Dentler, J. Kopp and N. Saviano, *Sterile neutrinos with secret interactions — cosmological discord?*, *JCAP* **11** (2018) 049 [arXiv:1806.10629] [INSPIRE].

[68] A. Mazumdar, S. Mohanty and P. Parashari, *Inflation models in the light of self-interacting sterile neutrinos*, *Phys. Rev. D* **101** (2020) 083521 [arXiv:1911.08512] [INSPIRE].

[69] C. Jarlskog, *Commutator of the quark mass matrices in the standard electroweak model and a measure of maximal CP-violation*, *Phys. Rev. Lett.* **55** (1985) 1039 [INSPIRE].

[70] Y. Reyimuaji and C. Liu, *Prospects of light sterile neutrino searches in long-baseline neutrino oscillations*, *JHEP* **06** (2020) 094 [arXiv:1911.12524] [INSPIRE].

[71] P. Bamert, C.P. Burgess and R.N. Mohapatra, *Heavy sterile neutrinos and neutrinoless double beta decay*, *Nucl. Phys. B* **438** (1995) 3 [hep-ph/9408367] [INSPIRE].

[72] P. Benes, A. Faessler, F. Simkovic and S. Kovalenko, *Sterile neutrinos in neutrinoless double beta decay*, *Phys. Rev. D* **71** (2005) 077901 [hep-ph/0501295] [INSPIRE].

[73] I. Esteban et al., *NuFIT 3.2* (2018).

[74] S. Gariazzo, C. Giunti, M. Laveder, Y.F. Li and E.M. Zavanin, *Light sterile neutrinos*, *J. Phys. G* **43** (2016) 033001 [arXiv:1507.08204] [INSPIRE].

[75] A. Bandyopadhyay, S. Choubey, S. Goswami and S.T. Petcov, *High precision measurements of θ(solar) in solar and reactor neutrino experiments*, *Phys. Rev. D* **72** (2005) 033013 [hep-ph/0410283] [INSPIRE].

[76] A. Bandyopadhyay, S. Choubey and S. Goswami, *Exploring the sensitivity of current and future experiments to θ(solar)*, *Phys. Rev. D* **67** (2003) 113011 [hep-ph/0302243] [INSPIRE].

[77] KAMLAND-ZEN collaboration, *Search for Majorana neutrinos near the inverted mass hierarchy region with KamLAND-Zen*, *Phys. Rev. Lett.* **117** (2016) 082503 [*Addendum ibid.* **117** (2016) 109903] [arXiv:1605.02889] [INSPIRE].

[78] P.F. Harrison and W.G. Scott, *μ-τ reflection symmetry in lepton mixing and neutrino oscillations*, *Phys. Lett. B* **547** (2002) 219 [hep-ph/0210197] [INSPIRE].

[79] P.F. Harrison and W.G. Scott, *Symmetries and generalizations of tri-bimaximal neutrino mixing*, *Phys. Lett. B* **535** (2002) 163 [hep-ph/0203209] [INSPIRE].

[80] W. Grimus and L. Lavoura, *A nonstandard CP transformation leading to maximal atmospheric neutrino mixing*, *Phys. Lett. B* **579** (2004) 113 [hep-ph/0305309] [INSPIRE].

[81] F. Feruglio, C. Hagedorn and R. Ziegler, *Lepton mixing parameters from discrete and CP symmetries*, *JHEP* **07** (2013) 027 [arXiv:1211.5560] [INSPIRE].

[82] P.F. Harrison and W.G. Scott, *The simplest neutrino mass matrix*, *Phys. Lett. B* **594** (2004) 324 [hep-ph/0403278] [INSPIRE].

[83] W. Rodejohann and X.-J. Xu, *Trimaximal μ-τ reflection symmetry*, *Phys. Rev. D* **96** (2017) 055039 [arXiv:1705.02027] [INSPIRE].

[84] D. Borah, M.K. Das and A. Mukherjee, *Common origin of nonzero $θ_{13}$ and baryon asymmetry of the Universe in a TeV scale seesaw model with A_4 flavor symmetry*, *Phys. Rev. D* **97** (2018) 115009 [arXiv:1711.02445] [INSPIRE].

[85] R. Krishnan, *TM_1 neutrino mixing with $\sin θ_{13} = \frac{1}{\sqrt{3}} \sin \frac{\pi}{12}$*, arXiv:1912.02451 [INSPIRE].

[86] S.F. King and M. Malinsky, *A_4 family symmetry and quark-lepton unification*, *Phys. Lett. B* **645** (2007) 351 [hep-ph/0610250] [INSPIRE].

[87] R. Gonzalez Felipe, H. Serodio and J.P. Silva, *Neutrino masses and mixing in A_4 models with three Higgs doublets*, *Phys. Rev. D* **88** (2013) 015015 [arXiv:1304.3468] [INSPIRE].

[88] S. Pramanick and A. Raychaudhuri, *Three-Higgs-doublet model under A_4 symmetry implies alignment*, *JHEP* **01** (2018) 011 [arXiv:1710.04433] [INSPIRE].